Journal of Photochemistry and Photobiology A: Chemistry 217 (2011) 369–375

Contents lists available at ScienceDirect

Journal of Photochemistry and Photobiology A: Chemistry

journal homepage: www.elsevier.com/locate/jphotochem

Room temperature hydrolysis of lumiflavin in alkaline aqueous solution

A. Penzkofer[a,*], A. Tyagi[a], J. Kiermaier[b]

[a] Fakultät für Physik, Universität Regensburg, Universitätsstrasse 31, D-93053 Regensburg, Germany
[b] Fakultät für Chemie und Pharmazie, Universität Regensburg, Universitätsstrasse 31, D-93053 Regensburg, Germany

ARTICLE INFO

Article history:
Received 7 June 2010
Received in revised form
11 November 2010
Accepted 14 November 2010
Available online 23 November 2010

Keywords:
Lumiflavin
Alkaline hydrolysis dynamics
Quinoxaline derivatives
7,8-Dimethyl-isoalloxazine
Methyl-isoalloxazine
Absorption cross-section spectra
Fluorescence quantum distributions
Fluorescence lifetimes
Hydrolysis rate constants

ABSTRACT

The degradation of lumiflavin (7,8,10-trimethyl-isoalloxazine, LF) in aqueous 1–4 M sodium hydroxide solutions (pH 14–14.6) at room temperature in the dark was studied by absorption spectroscopy, fluorescence spectroscopy, and mass spectrometry. Absorption cross-section spectra, fluorescence quantum distributions, fluorescence quantum yields, and fluorescence lifetimes at certain times after sample preparation were determined. The degradation products were analyzed by combined liquid chromatography and mass spectrometry. Lumiflavin is present in anionic form (LF^-). It degrades to anionic 7,8-dimethyl-isoalloxazine ($DMIA^-$), anionic methyl-isoalloxazine (MIA^-), and to the quinoxaline derivatives of 1,2-dihydro-2-keto-1,6,7-trimethyl-quinoxaline-3-carboxylic acid (QO1), 2-methoxy-6,7-dimethyl-quinoxaline-3-carboxylic acid (QO2), methyl-quinoxaline-2-ol (QO3), and 3-hydroxy-1,6,7-trimethyl-1*H*-quinoxaline-2-one (QO4). The rate constants of the NaOH catalyzed lumiflavin degradation are determined for the investigated samples.

1. Introduction

Lumiflavin (7,8,10-trimethyl-isoalloxazine, LF) is a member of the huge class of flavins [1,2]. It is the photoproduct of riboflavin (RF), flavin mononucleotide (FMN), and flavin adenine dinucleotide (FAD) in alkaline solution (pH >9) [1,2]. The photo-physical behaviour of lumiflavin is described in [1–5] and references therein. The pH dependence of absorption and emission was studied in [5–8] and ionization equilibria between cationic and neutral forms ($pK_c = 0.38$), as well as between neutral and anionic forms ($pK_a = 10.8$) were determined [5].

The photo-stability of lumiflavin in aqueous solutions [3,9,10], organic solvents [3,9,11], and in biological matter [12–16] was investigated. In alkaline solution at elevated temperatures lumiflavin was found to be unstable [17–24]. Hydrolysis products of lumiflavin (LF, $C_{13}H_{12}N_4O_2$) were found to be 1,2-dihydro-2-keto-1,6,7-trimethyl-quinoxaline-3-carboxylic acid (QO1, $C_{12}H_{12}N_2O_3$), 1,2-dihydro-2-keto-1,6,7-trimethyl-quinoxaline (Q, $C_{11}H_{12}N_2O$), urea ($H_2N–CO–NH_2$) and CO_2 [18,24] according to the reactions (a) $LF + 2H_2O \rightarrow QO1 + \text{urea}$, and (b) $QO1 \rightarrow Q + CO_2$ [18]. Thermal hydrolysis of flavins to quinoxaline derivatives and urea in alkaline solutions is not limited to lumiflavin. It was observed and studied on the yellow oxidation ferment (FMN as cofactor of the enzyme) [25,26], on riboflavin [17,18,27–30], D- and L-arabinoflavin [24]. The 1,2-dihydro-6,7-dimethyl-2-keto-1-D-ribityl-quinoxaline-3-carboxylic acid from riboflavin alkaline hydrolysis has a depressant action on cardiac and visceral muscles when injected intravenously [24].

Recently we studied the pH dependent absorption and emission behaviour of lumiflavin [5] in aqueous solutions in the range from pH −1.08 to 14.6. For pH ≥14 we observed spectral changes with time at room temperature. The observed temporal degradation of lumiflavin in alkaline aqueous solution at high pH (≥14) initiated the studies presented in this paper.

We investigated the degradation of lumiflavin in 1 M, 2 M, and 4 M NaOH aqueous solutions at room temperature in the dark (pH range 14–14.6). In this high pH range LF is present completely in its anionic form LF^- [5–8,31]. The thermal degradation of LF^- was followed by absorption measurements at certain times. Fluorescence emission spectra excited at different wavelengths in the absorption region were recorded after complete conversion of lumiflavin in 4 M NaOH to degradation products. Luminflavin dissolved in 4 M NaOH after complete conversion to degradation products was analyzed by combined HPLC and electrospray mass spectrometry to help identifying the degradation products. Six degradation species are found with fluorescence maxima at 530 nm (anionic 7,8-

* Corresponding author at: Fakultät für Physik, Universität Regensburg, Universitätsstrasse 31, D-93053 Regensburg, Germany. Tel.: +49 941 943 2107; fax: +49 941 943 2754.
E-mail address: alfons.penzkofer@physik.uni-regensburg.de (A. Penzkofer).

1010-6030/$ – see front matter © 2010 Elsevier B.V. All rights reserved.
doi:10.1016/j.jphotochem.2010.11.007

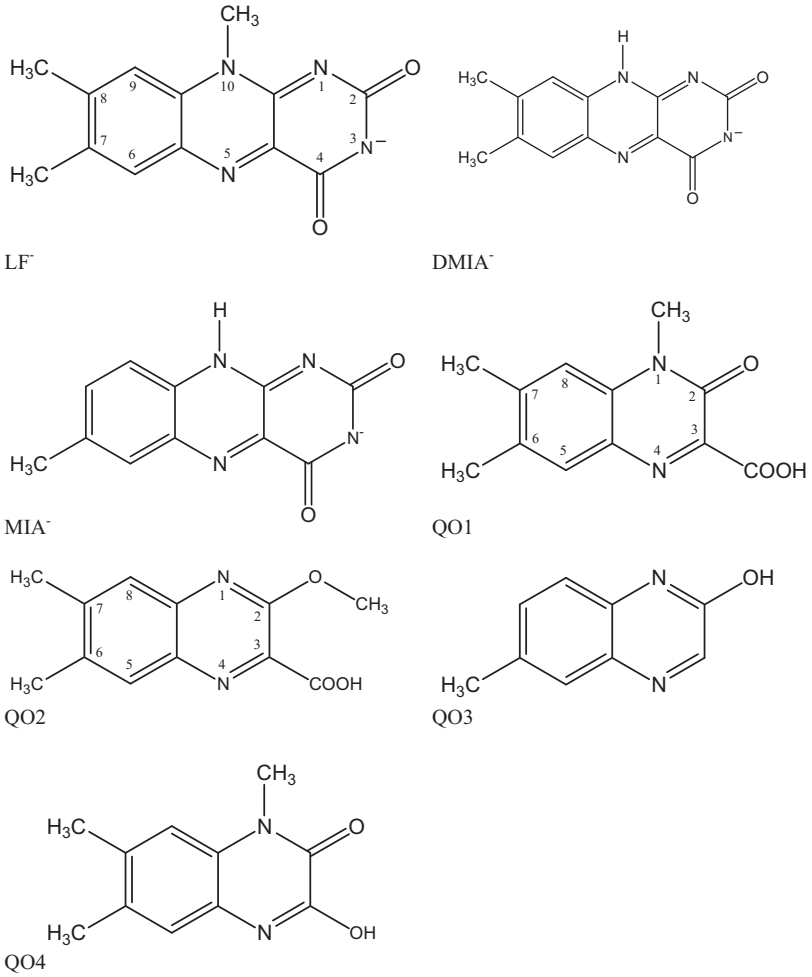

Fig. 1. Structural formulae of anionic lumiflavin (LF^-, sum formula $C_{13}H_{11}N_4O_2^-$, molar mass $M = 255.25$ Da), anionic 7,8-dimethyl-isoalloxazine ($DMIA^-$, $C_{12}H_9N_4O_2^-$, $M = 241.23$ Da), anionic 7-methyl-isoalloxazine (MIA^-, $C_{11}H_7N_4O_2^-$, $M = 227.20$ Da), 1,2-dihydro-2-keto-1,6,7-trimethyl-quinoxaline-3-carboxylic acid (QO1, $C_{12}H_{12}N_2O_3$, $M = 232.24$ Da), 2-methoxy-6,7-dimethyl-quinoxaline-3-carboxylic acid (QO2, $C_{12}H_{12}N_2O_3$, $M = 232.24$ Da), 6-methyl-quinoxaline-2-ol (QO3, $C_9H_8N_2O$, $M = 160.17$ Da), and 1-hydroxy-1,6,7-trimethyl-1*H*-quinoxaline-2-one (QO4, $C_{11}H_{12}N_2O_2$, $M = 204.23$ Da).

dimethyl-isoalloxazine, $DMIA^-$, [32] and 7-methyl-isoalloxazine or 8-methyl-isoalloxazine, MIA^-), 430 nm (1,2-dihydro-2-keto-1,6,7-trimethyl-quinoxaline-3-carboxylic acid, QO1 [18] and 3-hydroxy-1,6,7-trimethyl-1*H*-quinoxaline-2-one, QO4), 375 nm (2-methoxy-6,7-dimethyl-quinoxaline-3-carboxylic acid, QO2), and 305 nm (6-methyl-quinoxaline-2-ol or 7-methyl-quinoxaline-2-ol, QO3). Structural formulae of LF^-, $DMIA^-$, MIA^-, QO1, QO2, QO3, and QO4 are shown in Fig. 1. The hydrolysis product urea [17–22] absorbs weakly below 210 nm and therefore does not affect our absorption and emission spectroscopic studies in the excitation wavelength region from 220 nm to 480 nm.

2. Experimental

Lumiflavin (LF) was purchased from Sigma–Aldrich and used as delivered. The dye was dissolved in 1 M NaOH, 2 M NaOH, and 4 M NaOH (1 M = 1 mol dm^{-3}, the sodium hydroxide was dissolved in Millipore water, 1 M NaOH is the short-writing of 1 mol dm^{-3} NaOH in water). All measurements were carried out at room temperature under aerobic conditions. The samples were stored in the dark.

The absorption spectra were measured with a commercial spectrophotometer (Cary 50 from Varian). The fluorescence emission spectra were recorded with a commercial fluorimeter (Cary Eclipse from Varian) under magic angle conditions. The spectra were corrected for the spectral sensitivities of the detection system [33,34]. For absolute intrinsic fluorescence quantum distribution and quantum yield calibration the dyes lumiflavin in sodium phosphate buffer at pH 8 ($\phi_F = 0.29$ [5]) and POPOP (1,4-di(5-phenyloxazolyl)benzene) in ethanol ($\phi_F = 0.85$ [35]) were used as reference standards.

Time-resolved fluorescence traces were measured using second harmonic picosecond pulses at 400 nm of a mode-locked titanium-sapphire laser oscillator amplifier system (Hurricane from Spectra Physics) and an ultrafast streak-camera (type C1587 temporal disperser with M1952 high-speed streak unit from Hamamatsu) [36].

Combined high-pressure liquid chromatography–electrospray mass spectroscopy (HPLC–ES-MS) measurements were carried out with an Agilent 1100 HPLC system and a TSQ 7000 mass spectrometer from Thermo Quest Finnigan. The studied sample (lumiflavin in 4 M NaOH stored at room temperature in the dark for 150 days) was neutralized in acetic acid and extracted to dichloromethane. The used chromatographic column was Luna 2.5 μm, 50 mm × 2.1 mm, C18(2)-HST from Phenomenex, and the eluents were formic acid and acetonitrile (binary pump system used). The mass-spectrometer was operated with electrospray in positive ion mode.

3. Results

Apparent absorption cross-section spectra, $\sigma(\lambda)$, of the studied lumiflavin samples are shown in Fig. 2a-2c. They were calculated from measured transmission spectra ($\sigma = -\ln(T)/(\ell N_0)$, T:

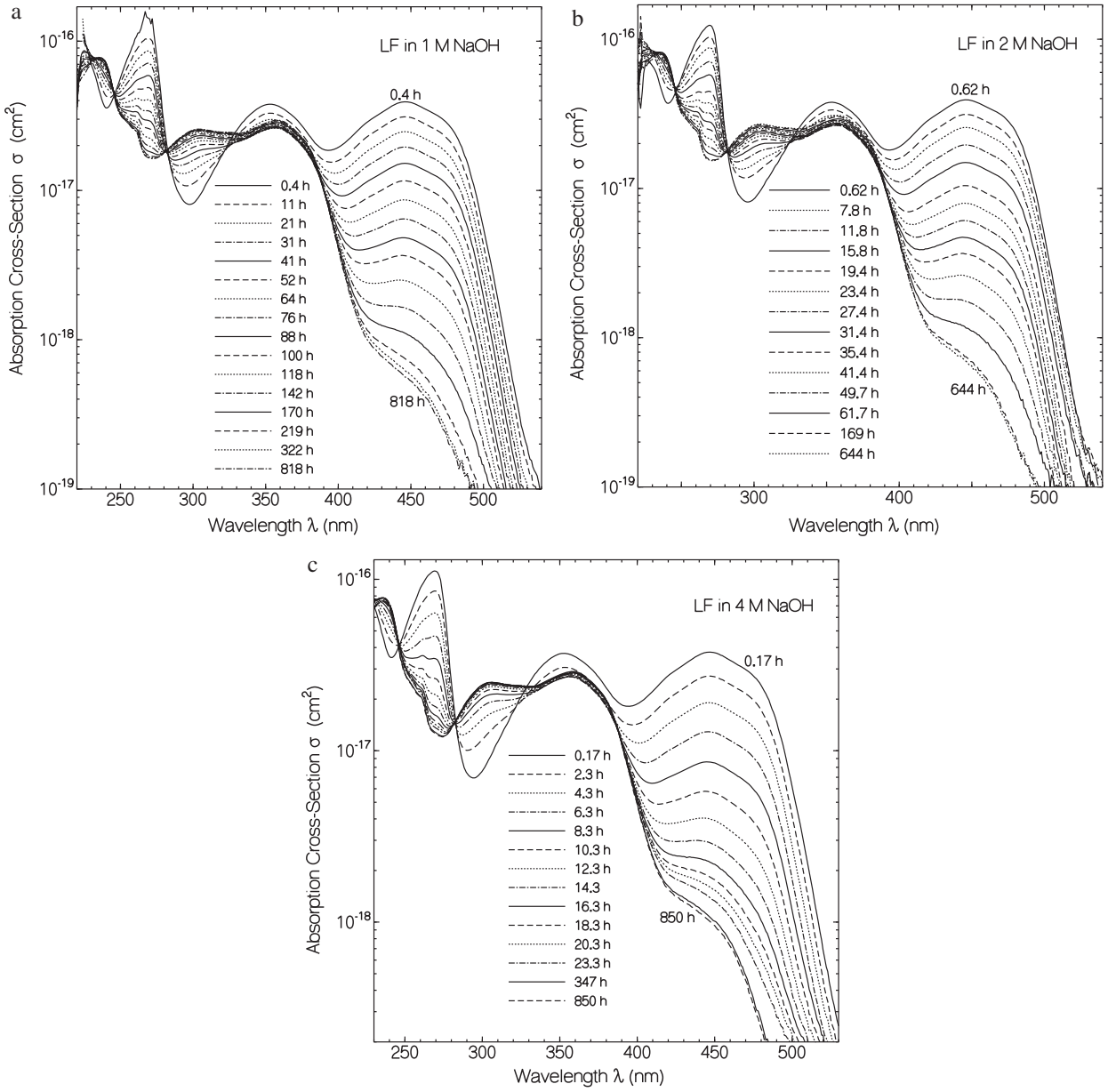

Fig. 2. Temporal development of absorption cross-section spectra of lumiflavin in (a) 1 M NaOH, (b) 2 M NaOH, and (c) 4 M NaOH at room temperature (≈21 °C). Storage times after preparation are listed in the legends.

transmission, ℓ: sample length, N_0: initial LF molecule number density). The LF concentration was in the range of 2×10^{-5} mol dm^{-3} to 5×10^{-5} mol dm^{-3}. The spectra were measured at certain times after sample preparation which are indicated in the figures. In part (a) the curves belong to LF in 1 M NaOH, in part (b) LF was dissolved in 2 M NaOH, and in part (c) the solvent was 4 M NaOH. In all three cases the absorption spectra changed similarly, only the speed of change was fastest for LF in 4 M NaOH and slowest for LF in 1 M NaOH. The long-wavelength absorption band around 450 nm decreased with time. Some pedestal absorption around 440 nm remained. The second absorption band around 350 nm was only slightly reduced. A new band around 300 nm was built up. The absorption of the band around 270 nm was lowered.

The absorption cross-section development at $\lambda_{pr} = 446$ nm versus storage time is shown in Fig. 3 for LF in 4 M NaOH (circles), 2 M NaOH (triangles), and 1 M NaOH (dots). At this wavelength only LF$^-$ and the hydrolysis products DMIA$^-$ and MIA$^-$ (see below reactions (R3) and (R4)) are absorbing. The absorption decrease is fitted by exponential decrease of the LF$^-$ absorption and exponential build-up of DMIA$^-$ and MIA$^-$ absorption according to

$$\sigma(t, \lambda_{pr}) = \sigma_{LF^-}(\lambda_{pr}) \exp\left(\frac{-t}{\tau_d}\right) + \sigma_{IA^-}(\lambda_{pr}) x_{IA^-,\infty} \left[1 - \exp\left(\frac{-t}{\tau_d}\right)\right], \quad (1)$$

In Eq. (1) IA$^-$ stands for DMIA$^-$ and MIA$^-$ (both compounds are thought to have a similar absorption cross-section spectrum). It is $\sigma_{LF^-}(\lambda_{pr}) = 3.93 \times 10^{-17}$ cm^2 [5] and $\sigma_{IA^-}(\lambda_{pr}) \approx \sigma_{DMIA^-}(\lambda_{pr}) = 2.62 \times 10^{-17}$ cm^2 [32]. The best fitting parameters are the degradation time constants τ_d (1 M NaOH) = 39 h, τ_d (2 M NaOH) = 13.5 h, τ_d (4 M NaOH) = 4.4 h, and the sum of the mole fractions of formed DMIA$^-$ and MIA$^-$ at infinite time of storage $x_{IA^-,\infty} = x_{DMIA^-,\infty} + x_{MIA^-,\infty} = 0.022$ for 1 M NaOH, $x_{IA^-,\infty} = 0.027$ for 2 M NaOH, and $x_{IA^-,\infty} = 0.039$ for 4 M NaOH. The time-constant of absorption degradation, τ_d, shortens over-proportional with increasing NaOH concentration, and the mole fraction of finally formed DMIA$^-$ and MIA$^-$ increases with NaOH concentration. The absorption reduc-

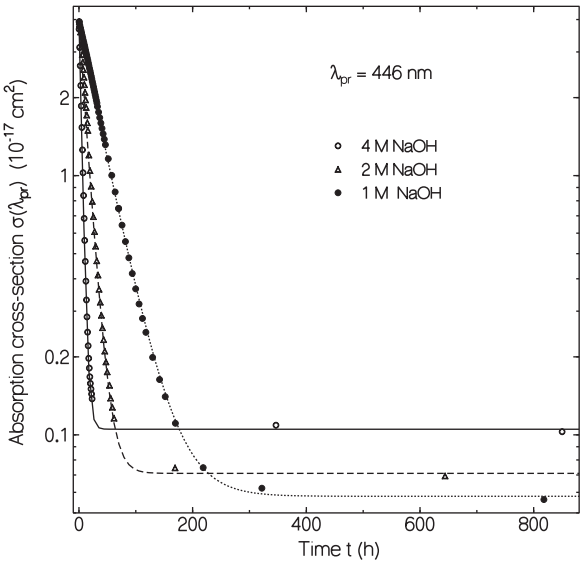

Fig. 3. Absorption cross-sections, σ(446 nm), versus storage time at room temperature for lumiflavin in 1 M NaOH (dots), 2 M NaOH (triangles), and 4 M NaOH (circles). Fitted curves are explained in the text.

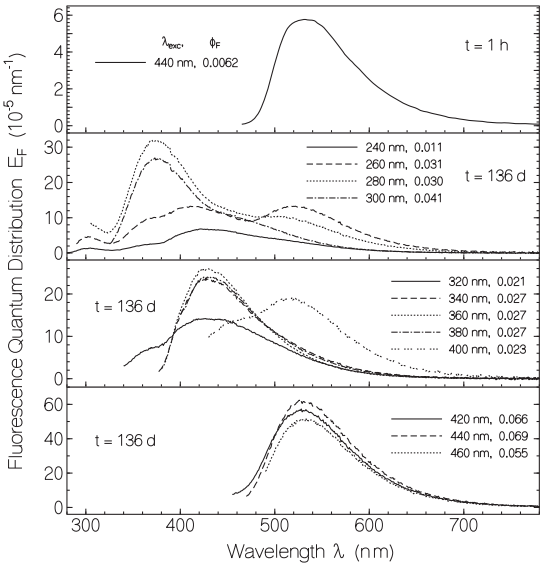

Fig. 5. Fluorescence quantum distributions of lumiflavin in 4 M NaOH stored at room temperature in the dark. Fluorescence excitation wavelengths, λ_{exc}, and obtained fluorescence quantum yields, ϕ_F, are listed in the sub-figures. The curve in the top part was measured 1 h after sample preparation. The other curves were measured 136 days after sample preparation.

tion at λ_{pr} = 446 nm is attributed to the degradation of lumiflavin to the quinoxaline derivatives QO1 [18], QO2, QO3, and QO4 (see reactions (R1), (R2), (R5), and (R6)) which are not absorbing at λ_{pr} = 446 nm.

In Fig. 4 absorption cross-section spectra of the original lumiflavin and of degradation products are shown. The solid curve shows the spectrum of freshly prepared lumiflavin in 1 M NaOH (pH 14). It is the absorption cross-section spectrum of LF^- (pK_a = 10.8 [5]). The dashed curve shows the absorption cross-section spectrum of $DMIA^-$ (taken from [32], the same spectrum is assumed for MIA^-). The dash-dotted curve shows the apparent absorption cross-section spectrum of the formed quinoxaline derivatives QO1, QO2, QO3, and QO4 which are abbreviated by QOs. It was obtained by subtracting the $DMIA^-$ and MIA^- contribution from the spectrum of lumiflavin in 4 NaOH after 818 h of storage and renormalization (i.e. $\sigma_{QOs}(\lambda) = [\sigma(\lambda, 818\,h, 4\,M\ \ NaOH) - x_{IA^-,\infty}\sigma_{DMIA^-}(\lambda)]/(1 - x_{IA^-,\infty})$ with $x_{IA^-,\infty} = 0.039$). The dotted curve shows the absorption cross-section spectrum of urea in water (from [37]).

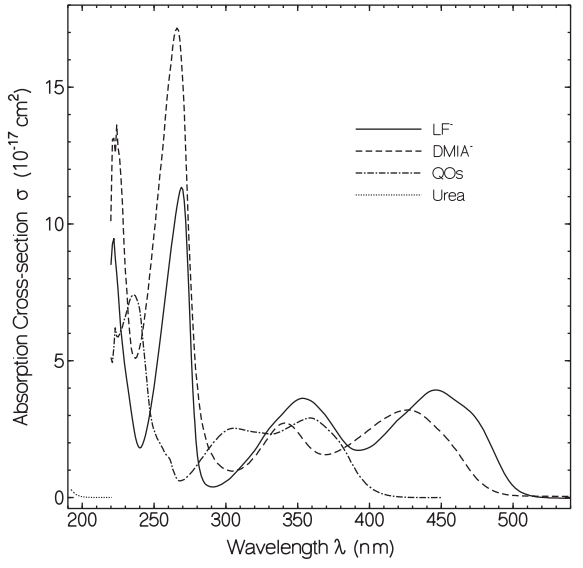

Fig. 4. Absorption cross-section spectra of LF^- (solid curve), $DMIA^-$ (dashed curve, from [32]), combined apparent absorption cross-section spectrum of QO1, QO2, QO3, and QO4 (dash-dotted curve, abbreviated by QOs), and absorption cross-section spectrum of urea in water (dotted curve, from [37]).

In Fig. 5 fluorescence quantum distributions of LF in 4 M NaOH are shown. The corresponding fluorescence quantum yields, $\phi_F = \int E_F(\lambda)\,d\lambda$, are listed in the sub-figures. The curve in the top part was measured 1 h after sample preparation. The fluorescence excitation occurred at λ_{exc} = 440 nm. The fluorescence signal belongs to LF^-. The obtained fluorescence quantum yield is ϕ_F = 0.0062. The other curves were measured 136 days after sample preparation whereby the sample was stored at room temperature in the dark. At that time lumiflavin was completely degraded. The excitation wavelength was varied in the range from λ_{exc} = 240 nm to 460 nm. The fluorescence quantum distributions depended on the excitation wavelength indicating the presence of at least four degradation products (fluorescence peaks around 305 nm, 375 nm, 430 nm and 530 nm).

In the lowest panel of Fig. 5 (excitation in the range λ_{exc} = 420–460 nm) the fluorescence is dominated by $DMIA^-$ and MIA^- emission. Maximum emission occurs at 530 nm. The fluorescence quantum yield is $\phi_F \approx 0.065$. The results are in good agreement with previous studies on $DMIA^-$ [32].

In the lower middle panel, for excitation in the range from 340 to 380 nm, the fluorescence is dominated by QO1 emission [24] with small QO4 contribution. The emission peaks at 430 nm. The fluorescence quantum yield is $\phi_F \approx 0.027$. The emission comes from the first absorption band of the quinoxaline derivatives (peak absorption at 360 nm, see dash-dotted curve in Fig. 4). Excitation at 400 nm results in a combined emission from QO1, QO4, $DMIA^-$, and MIA^-.

In the upper middle panel of Fig. 5 (excitation in the range of 240–300 nm) the fluorescence band peaking at 375 nm is attributed to QO2 emission. The emission comes from the second absorption band of the quinoxaline derivatives (peak absorption at 305 nm, see dash-dotted curve in Fig. 4). The fluorescence quantum yield of QO2 is roughly $\phi_F \approx 0.04$. For all excitation wavelengths from 240 nm to 300 nm, fluorescence contributions from QO2, QO1, QO4, $DMIA^-$ and MIA^- are present. Excitation at 240 nm and 260 nm shows the appearance of a weak fluorescence band peaking at 305 nm. This fluorescence band is attributed to the emission of QO3.

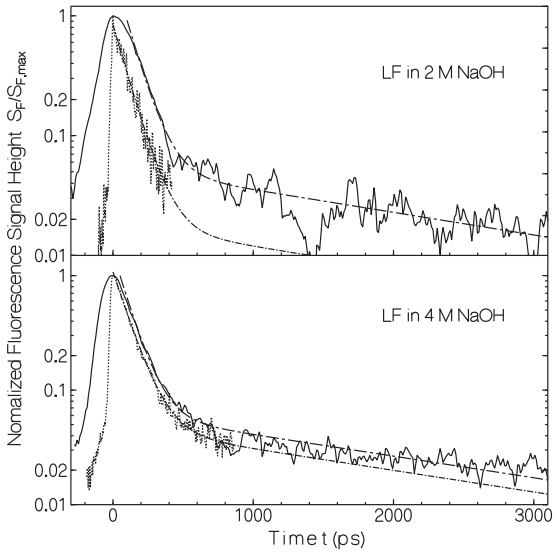

Fig. 6. Streak-camera fluorescence traces of lumiflavin in 2 M NaOH (top part) and in 4 M NaOH (bottom part) 2 to 3 h after sample preparation. Solid curves were measured with streak speed of 10 ps per pixel, and dotted curves were measured with streak speed of 1 ps per pixel. Dash-dotted curves are bi-exponential fits with short time constant of 105 ps and long time constant of 2.3 ns.

In Fig. 6 temporal fluorescence traces are shown for LF in 2 M NaOH (top part) and LF in 4 M NaOH (bottom part). The traces were measured 2–3 h after sample preparation. The samples were excited with 3 ps pulses at 400 nm and the fluorescence was collected in the range $\lambda_F > 500$ nm. The solid curves were measured with a streak speed of 10 ps per pixel, and the dotted curves were measured with a streak speed of 1 ps per pixel. The time resolutions are indicated by the rise times of the traces. Bi-exponential fluorescence decay is observed. The short decay component with a time constant of about 105 ps belongs to LF^- emission, and the long decay component with a time constant of about 2.3 ns belongs to emission from $DMIA^-$ and MIA^-. The determined lifetimes agree reasonably well with the fluorescence lifetimes of LF^- and $DMIA^-$ determined previously in [5,32], respectively.

Our LC–MS mass spectroscopic results on lumiflavin in Millipore water (diluted with acetonitrile for measurement) are shown in Fig. S1 of the supporting information. The top part of Fig. S1 shows the normalized total ion current (relative abundance) versus retention time t_{ret} (one peak at $t_{ret} = 4.60$ min). The mass spectrum at this retention time peak is shown in the lower part of Fig. S1. The main peak at $m/z = 257.0$ belongs to $[LF+H]^+$ (sum formula of lumiflavin: $C_{13}H_{12}N_4O_2$; molar mass of lumiflavin: $M = 256.26\,g\,mol^{-1}$). The peak at $m/z = 298.0$ is attributed to $[LF+MeCN+H]^+$ (MeCN = acetonitrile). The peak at $m/z = 513.1$ belongs to $[2LF+H]^+$.

Our LC–MS mass spectroscopic results on lumiflavin in 4 M NaOH stored at room temperature in the dark for 154 days are shown in Fig. S2 of the supporting information. There the top part shows the relative abundance versus retention time. Four peaks with retention times of $t_{ret} = 2.83$ min, 4.93 min, 5.03 min, and 5.45 min are found. The corresponding mass-spectra to these retention peaks are shown in the lower parts of Fig. S2. The mass spectrum at $t_{ret} = 2.83$ min gives a dominant peak at $m/z = 161.0$. It is attributed to 6-methyl-quinoxaline-2-ol and/or 7-methyl-quinoxaline-2-ol (QO3, sum formula $C_9H_8N_2O$, molar mass of $M = 160.17$ Da; 1 Da = 1 Dalton = $1\,g\,mol^{-1}$, structural formula is shown in Fig. 1, fluorescence peak around 305 nm). The small peaks at $m/z = 201.9$ and $m/z = 321.0$ belong to $[QO3+MeCN+H]^+$ and $[2QO3+H]^+$. The mass spectrum at $t_{ret} = 4.93$ min shows several peaks resulting from the component 7,8-dimethyl-isoalloxazine (DMIA, sum formula $C_{12}H_{10}N_4O_2$, molar mass $M = 242.24$ Da, structural formula depicted in Fig. 1, fluorescence peak around 530 nm). The observed mass peaks at $m/z = 242.9$, 284.0, 485.1, and 502.1 are assigned to $[DMIA+H]^+$, $[DMIA+MeCN+H]^+$, $[2DMIA+H]^+$, and $[2DMIA+NH_4]^+$, respectively. The mass spectrum to $t_{ret} = 5.03$ min is attributed to 7-methyl-isoalloxazine and/or 8-methyl-isoalloxazine (MIA) with molar mass $M = 228.21$ Da (sum formula $C_{11}H_8N_4O_2$, structural formula shown in Fig. 1, fluorescence peak around 530 nm) and 3-hydroxy-1,6,7-trimethyl-1*H*-quinoxaline-2-one (QO4) with molar mass $M = 204.23$ Da (sum formula $C_{11}H_{12}N_2O_2$, contribution to fluorescence peak at 430 nm). The mass peaks at $m/z = 229.0$, 270.0, and 457.2 are assigned to $[MIA+H]^+$, $[MIA+MeCN+H]^+$, and $[2MIA+H]^+$, respectively. The peaks at $m/z = 205.0$, 222.0 and 433.0 are assigned to $[QO4+H]^+$, $[QO4+NH_4]^+$, and $[QO4+MIA+H]^+$, respectively. The mass spectrum to $t_{ret} = 5.45$ min shows mass peaks at $m/z = 233.0$, 250.0, 465.0, and 482.1. They are attributed to $[M+H]^+$, $[M+NH_4]^+$, $[2M+H]^+$, and $[2M+NH_4]^+$, respectively. Thereby M stands for the two isomers 1,2-dihydro-2-keto-1,6,7-trimethyl-quinoxaline-3-carboxylic acid (QO1, sum formula $C_{12}H_{12}N_2O_3$, molar mass $M = 232.24$ Da, structural formula shown in Fig. 1, fluorescence peak around 430 nm) and 2-methoxy-6,7-dimethyl-quinoxaline-3-carboxylic acid (QO2, sum formula $C_{12}H_{12}N_2O_3$, molar mass $M = 232.24$ Da, structural formula shown in Fig. 1, fluorescence peak around 375 nm).

4. Discussion

The thermal lability of lumiflavin at high pH ($\geq$14) is clearly seen by the absorption spectra changes (Fig. 2) and the fluorescence spectra changes (Fig. 5). The hydrolysis of lumiflavin and riboflavin in alkaline solution at elevated temperature is documented in [17–30]. There only the formation of QO1 and some de-carboxylation of QO1 were resolved.

Our absorption, emission, and mass spectroscopic analysis reveals the hydrolysis of lumiflavin in strongly alkaline solution at room temperature into six components.

The dominant degradation products, QO1 and QO2, are formed by the hydrolysis processes (R1) [24] and (R2):

$$LF + 2H_2O \xrightarrow{NaOH} QO1 + \text{urea}. \quad (R1)$$

$$LF + 2H_2O \xrightarrow{NaOH} QO2 + \text{urea}. \quad (R2)$$

QO1 and QO2 have the same molar mass (Fig. S2 with retention time $t_{ret} = 5.45$ min), but their structural formulae, absorption spectra, and fluorescence spectra are different. A separation of the absorption cross-section spectra of QO1 and QO2 is not possible from the presented spectra (Fig. 2) since LF degrades in parallel into QO1 and QO2. Only the fluorescence spectra give a clear separation (fluorescence peaks at 430 nm and 375 nm). Semi-empirical quantum chemical calculations (PM3 method) indicate that the absorption peaking around 360 nm and the fluorescence peaking around 430 nm belong to QO1, and the absorption peaking around 305 nm and the fluorescence peaking around 375 nm belong to QO2.

The hydrolysis products $DMIA^-$ and MIA^- are thought to be formed by the processes (R3) and (R4):

$$LF^- + H_2O \xrightarrow{NaOH} DMIA^- + CH_3OH \quad (R3)$$

$$LF^- + 2H_2O \xrightarrow{NaOH} MIA^- + 2CH_3OH \quad (R4)$$

The components $DMIA^-$ and MIA^- cannot be distinguished from the measured absorption and fluorescence spectra because the absorbing and the emitting chromophore is in both cases the same. The presence of both components is seen in the LC–MS

mass-spectra of Fig. S2 (top part and mass spectra belonging to t_{ret} = 4.93 min and t_{ret} = 5.03 min).

The hydrolysis product QO3 is obtained by the formal reaction (R5):

$$LF + 4H_2O \xrightarrow{NaOH} QO3 + urea + CO_2 + 2CH_3OH. \quad (R5)$$

(see Fig. S2 with t_{ret} = 2.83 min). The absorption of QO3 is below 300 nm and its fluorescence is seen in a peak around 305 nm.

The hydrolysis product QO4 is obtained by the reaction process (R6):

$$LF + 2H_2O \xrightarrow{NaOH} QO4 + urea + CO. \quad (R6)$$

(see Fig. S2 with t_{ret} = 5.03 min and m/z = 205.0 for $[QO4+H]^+$). The absorption spectrum and fluorescence spectrum of QO4 is thought to coincide with those of QO1 because of the same chromophore part.

The formation of the degradation products, i, may be described by

$$\frac{dN_{LF^-}}{dt} = -\sum_i k_i N_{LF^-} = -k_{LF^-} N_{LF^-}, \quad (2)$$

$$\frac{dN_i}{dt} = k_i N_{LF^-}, \quad (3)$$

where N_{LF^-} is the number density of LF^-, and N_i is the number density of product i.

The solutions are

$$N_{LF^-} = N_0 \exp(-k_{LF^-} t), \quad (4)$$

$$N_i = \frac{k_i}{k_{LF^-}} N_0 [1 - \exp(-k_{LF^-} t)], \quad (5)$$

where N_0 is the initial number density of LF^-.

The degradation rate constant k_{LF^-} is obtained from the initial exponential absorption decrease in Fig. 3. The determined values are $k_{LF^-} = 7.2 \times 10^{-6}\,s^{-1}$ for LF in 1 M NaOH, $2.1 \times 10^{-5}\,s^{-1}$ for LF in 2 M NaOH, and $6.3 \times 10^{-5}\,s^{-1}$ for LF in 4 M NaOH. The constant k_{LF^-} increases with NaOH concentration as expected in a NaOH catalyzed reaction (transition state formation with NaOH involvement and subsequent NaOH release; see Michaelis–Menten kinetics [38]). The over-proportional increase of k_{LF^-} with NaOH concentration indicates some transition state activation barrier decrease with NaOH concentration. The transition state activation energy, E_A, may be estimated by the Arrhenius equation [39–42]:

$$k_{LF^-} \approx \frac{k_B \vartheta}{h} \exp\left(-\frac{E_A}{k_B \vartheta}\right) \quad (6)$$

where k_B is the Boltzmann constant, ϑ is the temperature, and h is the Planck constant. Using $k_{LF^-} = 6.3 \times 10^{-5}\,s^{-1}$ for LF in 4 M NaOH a value of $E_A \approx 8000\,cm^{-1}$ is estimated. The barrier height differences for the different NaOH concentrations may be estimated from the relation

$$\frac{k_{LF^-,NaOH1}}{k_{LF^-,NaOH2}} = \frac{[NaOH]_1 \exp(-(E_{A,1}/k_B\vartheta))}{[NaOH]_2 \exp(-(E_{A,2}/k_B\vartheta))} = \frac{[NaOH]_1}{[NaOH]_2} \exp\left(\frac{E_{A,2} - E_{A,1}}{k_B \vartheta}\right), \quad (7)$$

where the rate constant of degradation is set proportional to the NaOH concentration. The obtained transition state barrier height differences are $E_A(1\,M\ NaOH) - E_A(2\,M\ NaOH) \approx 77\,cm^{-1}$, and $E_A(1\,M\ NaOH) - E_A(4\,M\ NaOH) \approx 160\,cm^{-1}$.

The rate constant of LF^- degradation is composed of the rate constants of formation of the hydrolysis products, i.e. $k_{LF^-} = k_{QO1} + k_{QO2} + k_{QO3} + k_{QO4} + k_{DMIA^-} + k_{MIA^-} = k_{QOs} + k_{IA^-}$. For LF in 4 M NaOH the total degradation rate constant is $k_{LF^-} \approx 6.3 \times 10^{-5}\,s^{-1}$, the rate constant of $DMIA^-$ and MIA^- formation is $k_{IA^-} = x_{IA^-,\infty} k_{LF^-} \approx 2.5 \times 10^{-6}\,s^{-1}$ ($x_{IA^-,\infty} = 0.039$), and the rate constant of quinoxaline derivatives formation is $k_{QOs} = k_{LF^-} - k_{IA^-} \approx 6 \times 10^{-5}\,s^{-1}$.

5. Conclusions

The degradation of lumiflavin in aqueous 1 M, 2 M, and 4 M NaOH at room temperature in the dark was investigated by absorption, fluorescence, and mass spectroscopy. The hydrolysis of LF^- into the quinoxaline derivatives 1,2-dihydro-2-keto-1,6,7-trimethyl-quinoxaline-3-carboxylic acid QO1, 2-methoxy-6,7-dimethyl-quinoxaline-3-carboxylic acid QO2, methyl-quinoxaline-2-ol QO3, and 3-hydroxy-1,6,7-trimethyl-1*H*-quinoxaline-2-one QO4 and into the isoalloxazine derivatives 7,8-dimethyl-isoalloxazine DMIA and methyl-isoalloxazine MIA was revealed. The rate of degradation increased with NaOH (or OH^-) concentration. The time constant of hydrolysis was found to be 4.4 h for LF in 4 M NaOH, 13.5 h for LF in 2 M NaOH, 39 h for LF in 1 M NaOH, and it is expected to be ≥400 h for LF in aqueous solution at pH 13 (0.1 M NaOH).

Acknowledgements

The authors thank the Deutsche Forschungsgemeinschaft (DFG) for support in the Graduate College GK 640 "Sensory photoreceptors in natural and artificial systems" and in the Research Group FOR 526 "Sensory Blue Light Receptors". A.P. is grateful to Profs. F.J. Gießibl and J. Repp for their kind hospitality.

Appendix A. Supplementary data

Supplementary data associated with this article can be found, in the online version, at doi:10.1016/j.jphotochem.2010.11.007.

References

[1] P.F. Heelis, The photophysical and photochemical properties of flavins (isoalloxazines), Chem. Soc. Rev. 11 (1982) 15–39.
[2] F. Müller (Ed.), Chemistry and Biochemistry of Flavoenzymes, vol. 1, CRC Press, Boca Raton, FL, 1991.
[3] J. Kozoil, Studies on flavins in organic solvents—III. Spectral behaviour of lumiflavin, Photochem. Photobiol. 9 (1969) 45–53.
[4] E. Sikorska, I.V. Khmelinskii, J. Koput, M. Sikorski, Electronic structure of lumiflavin and its analogues in their ground and exited states, THEOCHEM 676 (2004) 155–165.
[5] A. Tyagi, A. Penzkofer, pH dependence of the absorption and emission behaviour of lumiflavin in aqueous solution, J. Photochem. Photobiol. A: Chem. 215 (2010) 108–115.
[6] C.H. Suelter, D.R. Metzler, The oxidation of a reduced pyridine nucleotide analog by flavins, Biochim. Biophys. Acta 44 (1960) 23–123.
[7] F. Kavanagh, R.H. Goodwin, The relationship between pH and fluorescence of several organic compounds, Arch. Biochem. 20 (1949) 315–324.
[8] K.H. Dudley, A. Ehrenberg, P. Hemmerich, F. Müller, Spektren und Strukturen der am Flavin-Redoxsystem beteiligten Partikeln, Helv. Chim. Acta 47 (1964) 1354–1383.
[9] J. Koziol, E. Knobloch, The solvent effect on the fluorescence and light absorption of riboflavin and lumiflavin, Biochim. Biophys. Acta 102 (1965) 289–300.
[10] W. Holzer, J. Shirdel, P. Zirak, A. Penzkofer, P. Hegemann, R. Deutzmann, E. Hochmuth, Photo-induced degradation of some flavins in aqueous solution, Chem. Phys. 308 (2005) 69–78.
[11] M. Green, G. Tollin, Flash photolysis of flavins. I. Photoreduction in non-aqueous solvents, Photochem. Photobiol. 7 (1968) 129–143.
[12] E. Choe, R. Huang, D.B. Min, Chemical reactions and stability of riboflavin in foods, J. Food Sci. 70 (2005) R28–R36.
[13] M.S. Grodowski, B. Veyret, K. Weiss, Photochemistry of flavins. II. Photophysical properties of alloxazines and isoalloxazines, Photochem. Photobiol. 26 (1977) 341–352.
[14] A. Yoshimura, T. Ohno, Lumiflavin-sensitized photooxygenation of indole, Photochem. Photobiol. 48 (1988) 561–565.
[15] M.Y. Jung, D.B. Min, ESR study of singlet oxygen quenching and protective activity of Trolox on the photodecomposition of riboflavin and lumiflavin in aqueous buffer solutions, J. Food Sci. 74 (2009) C449–C455.

[16] A. Knowles, E.M.F. Roe, A flash-photolysis investigation of flavin photosensitization of purine nucleotides, Photochem. Photobiol. 7 (1968) 421–436.
[17] R. Kuhn, H. Rudy, Th. Wagner-Jauregg, Über Lacto-flavin (vitamin B2), Ber. Deut. Chem. Ges. 66 (1933) 1950–1956.
[18] R. Kuhn, H. Rudy, Über den alkalilabilen Ring des Lacto-flavins, Ber. Deut. Chem. Ges. 67 (1934) 892–898.
[19] R. Kuhn, F. Bär, Zum photochemischen Verhalten des Lacto-flavins; Modellversuche in der Chinoxalin-Reihe, Ber. Deut. Chem. Ges. 67 (1934) 904–998.
[20] K.G. Stern, E.R. Holiday, Die Photo-flavine, eine Gruppe von Alloxazin-Derivaten, Ber, Deut. Chem. Ges. 67 (1934) 1442–1452.
[21] R. Kuhn, K. Reinemund, Über die Synthese des 6.7.9-trimethylflavins (Lumiflavins), Ber. Deut. Chem. Ges. 67 (1934) 1932–1936.
[22] J.W. Wellman, M. Tishler, 3,4-Dihydro-3-keto-4,6,7-trimethyl-2-quinoxalinecarboxylic acid, J. Am. Chem. Soc. 69 (1947) 714–715.
[23] R. Kuhn, H. Rudy, Über den alkali-labilen Ring des Lacto-flavins; Monomethyl- und Dimethylverbindungen, Berichte Deut. Chem. Ges. 67 (1934) 1125–1130.
[24] A.R. Surrey, F.C. Nachod, Alkaline hydrolysis of riboflavin, J. Am. Chem. Soc. 73 (1951) 2236–2238.
[25] O. Warburg, W. Christian, Über das gelbe Oxydationsferment, Biochem. Ztschr. 258 (1933) 496–498.
[26] O. Warburg, W. Christian, Über das gelbe Oxydationsferment, Biochem. Ztschr. 263 (1933) 228–229.
[27] H. Chick, H. Roscoe, Heat-stability of the (anti-dermatitis, "anti-pellagra") water-soluble vitamin B_2, Biochem. J. 24 (1930) 105–112.
[28] H. Chick, Copping, The heat-stability of the (anti-dermatitis, "anti-pellagra") water-soluble vitamin B_2. II, Biochem. J. 24 (1930) 932–938.
[29] R. Kuhn, Th. Wagner-Jauregg, Über die aus Eiklar und Milch isolierten Flavine, Ber. Deut. Chem. Ges. 66 (1933) 1577–1582.
[30] C. Daglish, N. Baxter, F. Wokes, The spectroscopy of riboflavine, Quart. J. Pharm. Pharmocol. 21 (1948) 898–904.
[31] S.G. Schulman, pH dependence of fluorescence of riboflavin and related isoalloxazine derivatives, J. Pharm. Sci. 60 (1971) 628–631.
[32] A. Tyagi, A. Penzkofer, Absorption and emission spectroscopic characterization of lumichrome in aqueous solutions, Photochem. Photobiol., doi:10.1111/j.1751-1097.2010.00836.x.
[33] A. Penzkofer, W. Leupacher, Fluorescence behaviour of highly concentrated rhodamine 6G solutions, J. Lumin. 37 (1987) 61–72.
[34] W. Holzer, M. Pichlmaier, A. Penzkofer, D.D.C. Bradley, W.J. Blau, Fluorescence spectroscopic behaviour of neat and blended conjugated polymer thin films, Chem. Phys. 246 (1999) 445–462.
[35] M. Mardelli, J. Olmsted III, Calorimetric determination of the 9,10-diphenyl-anthracene fluorescence quantum yield, J. Photochem. 7 (1977) 277–285.
[36] P. Zirak, A. Penzkofer, T. Mathes, P. Hegemann, Photo-dynamics of roseoflavin and riboflavin in aqueous and organic solvents, Chem. Phys. 358 (2009) 111–122.
[37] H.H. Perkampus, I. Sandeman, C.J. Timmons (Eds.), DMS UV Atlas of Organic Compounds, vol. II, Verlag Chemie, Weinheim, 1966, p. B11/1.
[38] D. Voet, J.G. Voet, Biochemistry, 3rd ed., John Wiley & Sons, 2004.
[39] G.R. Fleming, Chemical Applications of Ultrafast Spectroscopy, Oxford University Press, New York, 1986.
[40] J. Schmidt, A. Penzkofer, Absorption cross-sections, saturated vapor pressures, sublimation and evaporation energies of POPOP, dimethyl-POPOP and PPF vapors, J. Chem. Phys. 91 (1989) 1403–1409.
[41] M.G. Evans, M. Polanyi, Some applications of the transition state method to the calculation of reaction velocities, especially in solution, Trans. Faraday Soc. 31 (1935) 875–894.
[42] H. Eyring, The activated complex in chemical reactions, J. Chem. Phys. 3 (1935) 107–115.